

1 **Photosynthetic acclimation and sensitivity to short- and long-term environmental changes**

2
3 **Authors:** Leonie Schönbeck^{1,2}, Charlotte Grossiord^{1,2}, Arthur Gessler^{3,4}, Jonas Gisler³, Katrin
4 Meusburger⁵, Petra D'Odorico³, Andreas Rigling^{3,4}, Yann Salmon^{6,7}, Benjamin D. Stocker^{3,4},
5 Roman Zweifel³, Marcus Schaub³

6 ¹Plant Ecology Research Laboratory, School of Architecture, Civil and Environmental
7 Engineering, EPFL, Station 2, 1015 Lausanne, Switzerland

8 ²Functional Plant Ecology, Community Ecology Unit, Swiss Federal Institute for Forest, Snow
9 and Landscape Research WSL, Station 2, 1015 Lausanne, Switzerland

10 ³Forest Dynamics Research Unit, Swiss Federal Research Institute for Forest, Snow and
11 Landscape Research WSL, Zürcherstrasse 111, 8903 Birmensdorf, Switzerland

12 ⁴Department of Environmental Systems Science, ETH Zürich, Universitätstrasse 2, 8092
13 Zürich, Switzerland

14 ⁵Biogeochemistry Unit, Swiss Federal Research Institute for Forest, Snow and Landscape
15 research WSL, Zürcherstrasse 111, 8903 Birmensdorf, Switzerland

16 ⁶Institute for Atmospheric and Earth System Research/Forest Sciences, University of Helsinki,
17 P.O. Box 27, 00014 University of Helsinki, Finland

18 ⁷Institute for Atmospheric and Earth System Research/Physics, University of Helsinki, P.O.
19 Box 68, 00014 University of Helsinki, Finland

20 21 **Figures (5 – Full color):**

22 Fig. 1. Experimental design.

23 Fig. 2. Meteorological and soil water data.

24 Fig. 3. Boxplots of long-term acclimation of A , g_s , E , WUE_i , V_{Cmax} , J_{max} .

25 Fig. 4. Sensitivity of g_s to environmental changes.

26 Fig. 5. Acclimation process of gas exchange in irrigation-stop trees after 11 years of irrigation.

27 28 **Supporting information (3 Figures, full color, 4 Tables)**

29 Fig. S1. VPD inside and outside the cuvette

30 Fig. S2. Sensitivity parameter m and rasterplot of g_s in control and irrigated trees

31 Fig. S3. Absolute values of gas exchange parameters during acclimation in control and irrigated
32 trees

33 Table S1. Parameters for A/C_i fitting

34 Table S2. Mean values of gas exchange parameters in control, irrigated and irrigation-stop trees
35 per year

36 Table S3. Anova results of linear mixed effect model for g_s sensitivity

37 Table S4. Model coefficients for g_s as a function of soil VWC and VPD

38

39 **Summary**

- 40 • The future climate will be characterized by an increase in frequency and duration of
41 drought and warming that exacerbates atmospheric evaporative demand. How trees
42 acclimate to long-term soil moisture changes and whether these long-term changes alter
43 trees' sensitivity to short-term (day to months) variations of vapor pressure deficit
44 (VPD) and soil moisture is largely unknown.
- 45 • Leaf gas exchange measurements were performed within a long-term (17 years)
46 irrigation experiment in a Scots pine-dominated forest in one of Switzerland's driest
47 areas on trees in naturally dry (control), irrigated, and 'irrigation-stop' (after 11 years of
48 irrigation) conditions.
- 49 • Seventeen years of irrigation increased photosynthesis (A) and stomatal conductance
50 (g_s) and reduced the g_s sensitivity to increasing VPD but not to soil drying. Following
51 irrigation-stop, gas exchange did not decrease immediately, but after three years, had
52 decreased significantly in irrigation-stop trees. $V_{C_{max}}$ and J_{max} recovered after five years.
- 53 • These results suggest that long-term release of soil drought reduces the sensitivity to
54 atmospheric evaporative demand and that atmospheric constraints may play an
55 increasingly important role in combination with soil drought. In addition, they suggest
56 that structural adjustments lead to an attenuation of initially strong leaf-level
57 acclimation to strong multiple-year drought.

58 **Keywords:** A/Ci, photosynthesis, gas exchange, sensitivity, drought, acclimation, stomatal
59 conductance, VPD

60 **Introduction**

61 Many temperate ecosystems will experience an increase in frequency and intensity of both soil
62 and atmospheric drought due to changing precipitation patterns and increasing temperatures
63 that exacerbate atmospheric evaporative demand (higher vapor pressure deficit, VPD)
64 (Simmons *et al.*, 2010; Willett *et al.*, 2014). To date, it is poorly understood how these combined
65 stressors affect tree productivity, specifically how they affect the photosynthetic machinery of
66 trees.

67 Knowledge of species-specific traits related to carbon assimilation and water consumption is
68 crucial to assess and predict tree and forest functioning. Terrestrial biosphere models (TBMs)
69 commonly use prescribed and temporally constant traits for a discrete set of plant functional
70 types to specify photosynthetic capacity. The Farquhar, von Caemmerer and Berry (FvCB)
71 model is widely used for mechanistically simulating photosynthesis (Farquhar *et al.*, 1980) as
72 a function of photosynthetic capacities – Rubisco carboxylation ($V_{c_{max}}$) and electron transport
73 (J_{max}). In addition, it relies on stomatal conductance (g_s) and its sensitivity to the environment,
74 which need to be estimated empirically or by modelling approaches funded in optimality
75 principles for balancing carbon gains and water losses (Wang *et al.*, 2020; Prentice *et al.*, 2014;
76 Medlyn *et al.*, 2011; Wright & Westoby, 2003; Cowan & Farquhar, 1977). Common to most
77 stomatal optimization models and the state-of-the-art in global TBMs is that $V_{c_{max}}$ and J_{max} are
78 assumed to be constants when expressed at a standard temperature and do not respond to
79 varying soil moisture or VPD (Medlyn *et al.*, 2002; Egea *et al.*, 2011; De Kauwe *et al.*, 2013).
80 Yet, empirical evidence in saplings and relative short-term experiments exists for acclimating
81 responses in $V_{c_{max}}$ and J_{max} , e.g., during progressively drying soil conditions (Zhou *et al.*, 2014).
82 However, the lack of long-term data on adult trees hampers our ability to estimate drought
83 impacts and understand the susceptibility and capacity for acclimation of plant carbon
84 assimilation.

85 Short-term acclimation occurs when trees adjust their physiology to overcome slowly
86 increasing stresses (Kozlowski and Pallardy, 2002; Marchin *et al.*, 2016; Grossiord *et al.*, 2018).
87 Stomata regulate the balance between carbon intake and water loss. They will close (g_s
88 decreases) when trees experience soil or atmospheric drought, which will reduce transpiration
89 (E), CO_2 diffusion, and CO_2 concentration inside the leaf (C_i). Lower C_i , in turn, causes reduced
90 leaf-level photosynthetic activity (A). Drought could also lead to a decrease in Rubisco activity,
91 down-regulating the activation state of the enzyme, leading to a reduction in Rubisco content
92 and/or soluble protein content (Parry, 2002). While stomatal closure, and thus stomatal

93 limitation, is purely affecting diffusion of CO₂ and water vapor, other processes, summarized
94 as non-stomatal limitation of photosynthesis, affect the diffusion of CO₂ through the mesophyll,
95 and the photo- and biochemistry of photosynthesis. For example, the downregulation of
96 Rubisco can be considered as a non-stomatal but biochemical limitation of the photosynthetic
97 capacity during drought, leading to reduced V_{cmax} and J_{max} (Kanechi *et al.*, 1996; Wilson *et al.*,
98 2000; Castrillo *et al.*, 2001; Parry, 2002; Tezara, 2002; Zhou *et al.*, 2014). Moreover, mesophyll
99 conductance (g_m) can exert a diffusional but non-stomatal limitation on photosynthesis, and,
100 depending on the species, increases, decreases or doesn't change at all in response to drought
101 (Hommel *et al.*, 2014). Several studies found that deciduous tree species during drought mainly
102 showed stomatal limitation of A (Wilson *et al.*, 2000; Flexas *et al.*, 2004; Keenan *et al.*, 2010),
103 while other studies found that the effect size of the two limitations is strongly dependent on tree
104 species, habitat, and duration of drought (Zhou *et al.*, 2013, 2014; Salmon *et al.*, 2020)..

105 Stomatal and biochemical acclimation could be achieved on a timescale from minutes to weeks,
106 whereas structural acclimation, such as adjustment of root-to-leaf ratio or leaf-to-sapwood area,
107 could take multiple years (Sultan, 2000; Poyatos *et al.*, 2007; Martínez-Vilalta *et al.*, 2009).
108 Long-term structural changes can alter the sensitivity of the stomata and photosynthetic
109 apparatus to short-term fluctuations in the environment (e.g. Gessler *et al.*, 2017). For example,
110 a high ratio of leaf-to-sapwood area resulting from acclimation to high soil water availability
111 allows for similar C assimilation with increased water loss (Zweifel *et al.*, 2020) but may pose
112 a hydraulic risk during sudden heatwaves with strong atmospheric demand, causing the stomata
113 to close rapidly. Moreover, a reduced ratio of root-to-leaf area might expose the tree to greater
114 risk during extreme and enduring soil drought. In contrast, trees acclimated to low soil water
115 content perform a more conservative water use. Their lower leaf area reduces total tree water
116 loss while enabling leaves to maintain their function with normal g_s and A (Pataki *et al.*, 1998;
117 Kelly *et al.*, 2016). They might capitalize on sudden increases in soil water, while their posture
118 with smaller leaf area will probably not react as strongly on fluctuations in evaporative demand.
119 Also, V_{cmax} and J_{max} might be prone to acclimation where acclimation to aridity might lead to
120 significantly more protein allocated to Rubisco in leaves (Pankovic *et al.*, 1999; Wright *et al.*,
121 2003; Prentice *et al.*, 2014; Wang *et al.*, 2017). Still, how exactly photosynthetic acclimation to
122 changing soil moisture proceeds, and how acclimation affects the sensitivity of g_s to short-term
123 environmental fluctuations is unknown.

124 There is an increasing need to characterize tree physiological sensitivity and acclimation to
125 atmospheric and soil drought (Grossiord *et al.*, 2020). Measuring leaf-level photosynthetic
126 capacity and sensitivity to environmental cues is time-consuming but indispensable for

127 answering to which extend trees respond to drought over the long *vs.* the short term. Although
128 leaf-level gas exchange measurements have been conducted on multiple species, no study has
129 yet attempted to decipher how long-term exposure to soil moisture change, and subsequent
130 adjustments to novel conditions, could alter the sensitivity of photosynthetic properties to
131 environmental variability. In a Scots pine-dominated forest in one of Switzerland's driest areas,
132 we conducted leaf-level gas exchange measurements in a long-term irrigation experiment
133 covering multiple years. We tested (1) how photosynthetic properties (i.e., A , g_s , J_{max} , and
134 $V_{c_{max}}$) acclimate in response to long-term (17 years) artificial change in soil moisture (naturally
135 drought-exposed control trees *vs.* irrigated trees), (2) how acclimation to long-term changes in
136 soil moisture impacts the sensitivity of photosynthetic properties to short-term VPD and soil
137 moisture variation, and (3) how fast photosynthetic properties of trees recover when drought
138 follows a long-term acclimation to high soil moisture (irrigation stopped after 11 years). We
139 hypothesized that (1) acclimation to long-term irrigation had led to similar A , g_s , $V_{c_{max}}$ and J_{max}
140 and lower intrinsic water use efficiency (WUE_i) compared to control trees, due to structural
141 acclimation; (2) irrigated trees will show stronger sensitivity to atmospheric drivers due to their
142 sizeable water-consuming crown, while control trees will react stronger to soil moisture
143 fluctuations; (3) trees released from the irrigation and exposed to sudden drought (irrigation-
144 stop) will strongly reduce their photosynthetic properties in the first year, followed by structural
145 adjustments (e.g., lower crown leaf area and water-conducting area) that allow for a recovery
146 of leaf-level gas exchange.

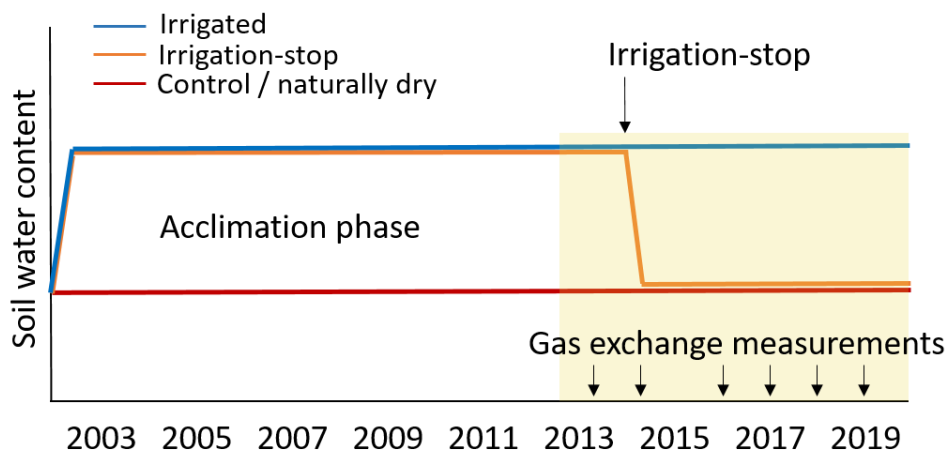
147 **Materials and Methods**

148 *Site and experimental design*

149 A 17-year irrigation experiment was conducted in the Pfywald forest (46°18N, 7°36' E, 615
150 m a.s.l.), the largest Scots pine (*Pinus sylvestris* L.) dominated forest in Switzerland, located in
151 the dry inner-Alpine valley of the river Rhone, close to the dry edge of the natural distribution
152 of Scots pine (Critchfield and Little, 1966). The Pfywald is a 100-year-old naturally
153 regenerated forest, but past forest practices may have favored Scots pine regeneration over other
154 species such as *Quercus pubescens* (Weber *et al.*, 2008; Gimmi *et al.*, 2010; Rigling *et al.*,
155 2013). Climatic conditions are characterized by a mean annual temperature of 10.1 °C and a
156 yearly precipitation sum of approximately 600 mm. Scots pine forests in this region are
157 regularly subjected to drought- and heat-induced mortality (Bigler *et al.*, 2006; Allen *et al.*,
158 2010; Rigling *et al.*, 2013). The average tree age is approximately 100 years, and the forest has
159 a mean canopy height of 10.8 m, a stand density of 730 stems ha⁻¹, and a basal area of 27.3 m²

160 ha⁻¹ (Dobbertin *et al.*, 2010). The soil is a calcaric regosol (FAO classification) characterized
 161 by very low water retention and high vertical drainage (Brunner *et al.*, 2009).

162 The experimental site (1.2 ha; 800 trees) is divided into eight plots of 25 m x 40 m each,
 163 separated by a 5 m buffer zone. The irrigation of ~600 mm/year is applied at night on four plots
 164 between April and October, from 2003 onwards, with 1 m high sprinklers using water from a
 165 nearby channel running parallel to the experimental plot, fed by the Rhone River. Nutrient input
 166 through irrigation was proven to be minor (Thimonier *et al.*, 2005, 2010). In 2014, irrigation
 167 was stopped in the upper third of the irrigated plots, resulting in three categories: controls (non-
 168 irrigated) representing the natural dry condition; irrigation resulting in a release of soil drought;
 169 irrigation-stop exposing trees that were acclimated to well-watered conditions for 11 years to
 170 drought (Fig. 1). In 2015, nine scaffolds were installed in the forest, three per treatment, to
 171 enable easier access to tree crowns for sampling and *in situ* measurements. The volumetric soil
 172 water content (VWC) was monitored hourly in one control and one irrigated plot until 2014,
 173 using time domain reflectometry (Tektronix 1502B cable tester, Beaverton, OR, USA), at a soil
 174 depth of 10, 40, and 60 cm at four different locations per plot. In 2014, all soil moisture sensors
 175 were replaced with Decagon 10-HS sensors (Decagon Devices, Inc., Pullman, WA, USA). They
 176 were installed in six different plots (two irrigated, two control, and two irrigation-stop plots), at
 177 10 and 80 cm depth. Air temperature, relative humidity (Sensirion SHT-21, Sensirion AG,
 178 Switzerland), and precipitation (Tipping Bucket Rain Gauge, R.M. Young, MI USA) were
 179 measured on-site.



180
 181 **Figure 1:** Timeline of treatments and measurements from 2003 to 2019 in a long-term irrigation
 182 experiment. Irrigation was stopped in 2014 in 1/3 of the irrigated plots. Gas exchange measurements
 183 took place three times a year, from 2013 to 2019, except in 2015. In 2016, only control and irrigated
 184 trees were measured.

185 *Gas exchange measurements*

186 In 2013, 2014, and 2016-2019, leaf gas exchange measurements were carried out in the form
187 of A/C_i measurements. In 2013 and 2014, hunting seats were used on specific trees to access
188 fully sun-exposed branches of the outer upper crown for leaf-level gas exchange measurements.
189 In 2016, gas exchange was measured on branches cut off from sun-exposed parts in the upper
190 half of the canopy, cut again underwater, and kept in a bucket of water. In 2017-2019,
191 measurements were conducted from the top of the nine scaffolds and on three trees per scaffold.
192 Here, the top of the canopy was reached, and sun-exposed needles were selected for
193 measurements. Although measurements were taken from slightly different canopy depths but
194 always from sun-exposed branches from the outer crown, we assumed no strong gradients in
195 light, VPD, or other environmental conditions within the sparse canopy of the trees at our site.
196 In a Scots pine stand with a comparable structure, no intra-canopy gradients in gas exchange
197 were observed (Brandes *et al.*, 2006). Thus, we contend that the branches selected from the
198 outer crown were comparable and representative of the whole canopy. Until 2019,
199 measurements were carried out with two LiCor LI-6400 systems (LiCor Inc., Lincoln,
200 Nebraska, USA). The instruments were replaced by the LI-6800 system (LiCor Inc.) in 2019.
201 A/C_i measurements were taken once in spring (May/June), summer (July/August), and autumn
202 (October) of each year. Additional point measurements at 400 ppm CO₂ were taken in 2013,
203 2014, and in the summer of 2017, which were included in the analyses regarding A and g_s. Five
204 to 10 one-year-old (i.e., previous year) needles were enclosed clipped in the cuvette gasket,
205 ordered in a flat plane without overlapping each other. The temperature inside the cuvette was
206 set close to the outside midday temperature. With the LI-6800, VPD was set to 1.5 kPa, while
207 in the LI-6400, humidity regulation was not a built-in function, and RH was maintained between
208 60-70%. In most cases, this led to a decrease in VPD in the cuvette compared to outside
209 conditions (Supporting information Fig. S1). Nonetheless, the complete dataset comprises a
210 range of VPD values between 0.3 and 3 kPa. The actual conditions the needles experienced, i.e.
211 the cuvette VPD, was used as a covariate for statistical analyses. Photosynthetically active
212 radiation (PAR) was kept at saturation point of 1000-1200 μmol m⁻² s⁻¹ (Palmroth and Hari,
213 2001).

214 Photosynthetic activity was measured at CO₂ concentrations in the sequence steps of 400, 300,
215 200, 100, 50, 0, 400, 600, 800, 1200, and 1800 ppm. After each measurement, the part of the
216 needles enclosed in the cuvette was harvested, and the projected leaf area (Serrano *et al.*, 1997;
217 Renninger *et al.*, 2015) was measured using a flatbed scanner and analyzed using Pixstat

218 (Pixstat v1.3.0.0, Schleppei 2018). The projected leaf area of the measured foliage was used to
219 correct the recorded gas exchange values.

220 *A/C_i Curve fitting*

221 A/C_i curves were fitted using the Farquhar, von Caemmerer & Berry model for photosynthesis,
222 described in Sharkey et al. (2007) and computed in the ‘plantecophys’ package (Duursma,
223 2015). Before fitting, the data was cleaned based on visual determination to get rid of
224 unreasonable numbers due to measurement artifacts, following these criteria (Gu *et al.*, 2010):

- 225 - 0 ppm < C_i < 2000 ppm
- 226 - 0 mol/m²/s < g_s < 1.5 mol/m²/s
- 227 - -5 < A < 20 mmol/m²/s
- 228 - Each A/C_i curve must have reached a C_i of 600 ppm to ensure a saturating plateau
- 229 - A/C_i curve must have more than 5 points after the previous selection.

230 The ‘plantecophys’ package's default method was used if possible; all other fits were done with
231 the binomial method. The default assumption of infinite mesophyll conductance (g_m) was used.
232 As a result, ‘apparent’ V_{cmax} and J_{max} are computed, and changes in apparent V_{cmax} and J_{max}
233 reflect changes in both biochemical limitations as well as mesophyll conductance. The model
234 used a temperature correction to fit all curves to 25°C. Transition point, i.e. the C_i where the
235 transition takes place from Rubisco limited photosynthesis to RuBP regeneration/electron
236 transport limitation, was estimated by the model, as well as day respiration (R_d),
237 photorespiratory compensation point (Γ*) and the Michaelis-Menten Coefficient (K_m, Pa)
238 (Supplementary data Table S1). After fitting the curves, non-fitting curves were eliminated
239 following the following criteria based on validated values in the literature (von Caemmerer and
240 Farquhar, 1981; Wullschlegel, 1993; Gu *et al.*, 2010) and by visual determination of extreme
241 outliers:

- 242 - 0 ppm < Transition point (Tp) < 1600 ppm
- 243 - 3 μmol/m²/s < J_{max} < 150 μmol/m²/s
- 244 - 1 μmol/m²/s < V_{cmax} < 95 μmol/m²/s
- 245 - Root mean squared error (measure of accuracy) < 10

246 After cleaning, 213 out of 312 measured curves were considered in the analyses.

247 *Statistical analysis*

248 To test for general, long-term, treatment differences in A, g_s, E, intrinsic water use efficiency
249 (WUE_i, A/g_s), V_{cmax}, and J_{max}, a linear mixed effect model with the control and irrigated
250 treatment as fixed and tree individual nested in year as a random factor was used. The mixed

251 effect models were fitted using the ‘lmerTest’ package in R (Kuznetsova et al., 2017). The year
252 was also included as a fixed factor but never interacted with the treatment. It was thus chosen
253 to focus on the general treatment effect.

254 Linear mixed effect models were also used to test whether the long-term manipulation of soil
255 water changed the sensitivity of leaf g_s to short-term environmental variations. Only trees from
256 control and irrigated treatments were used for this analysis. The widely described relationship
257 between g_s and VPD was used as a basis for the g_s model. g_s is described using (Oren *et al.*,
258 1999):

$$259 \quad g_s = g_{s,\text{ref}} - m * \ln(\text{VPD}) \quad (1)$$

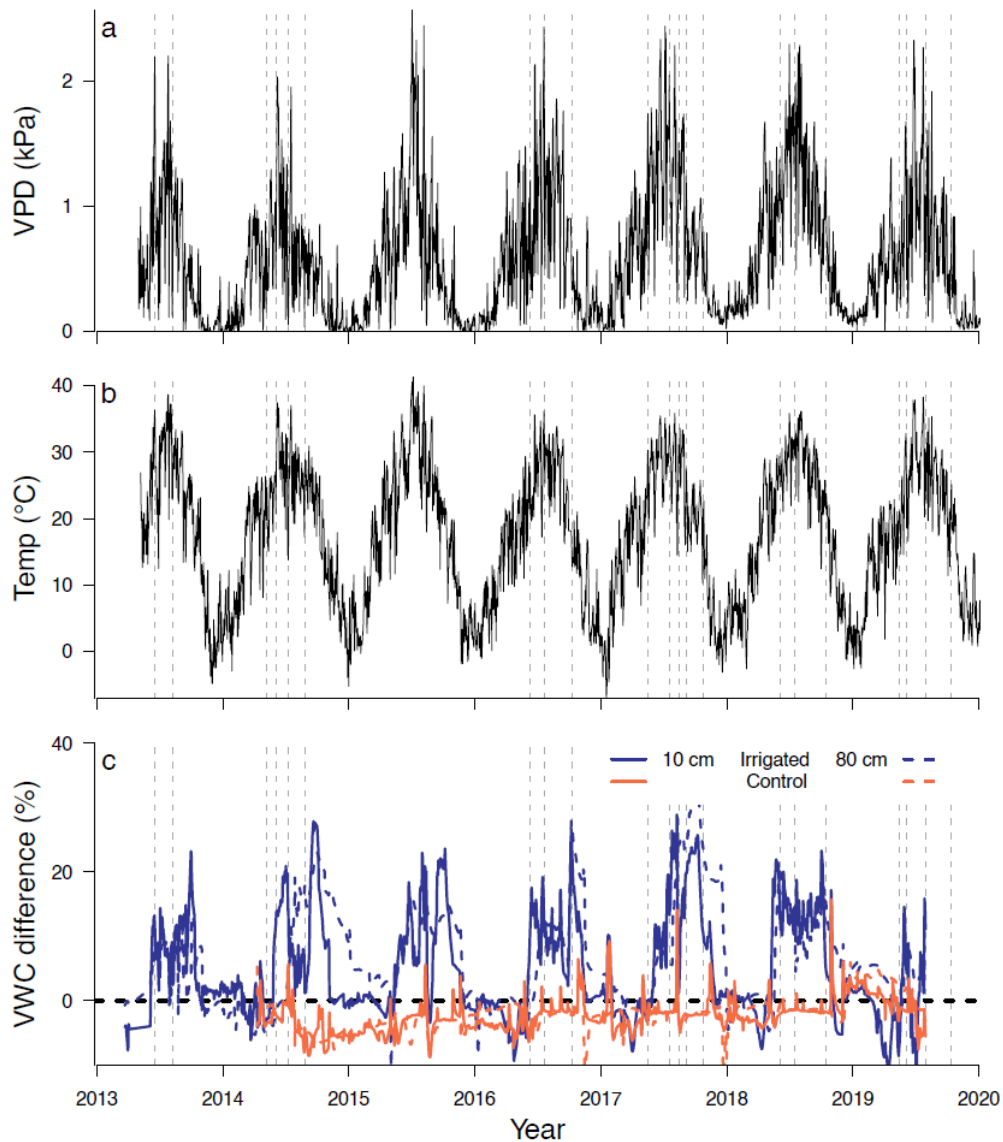
260 Where g_s is the stomatal conductance at any level of VPD, $g_{s,\text{ref}}$ is the reference stomatal
261 conductance at a VPD of 1 kPa, and m is the sensitivity of g_s to VPD. We then extended this
262 model with soil volumetric water content (2-degree polynomial) and treatment as fixed factors,
263 including all interactions, and tree nested in year as a random factor. Model selection was then
264 made according to the lowest Akaike information criterion (AIC). If needed, variables were
265 log- or square-root-transformed to meet the normal distribution of the residuals. For
266 visualization, three soil VWC bins were created, splitting the data up in soil VWC of 25-40%,
267 41-55%, and 56-70%. Modeled data were simulated using the ‘arm’ package (Gelman *et al.*,
268 2020).

269 Acclimation of all photosynthetic parameters previously described over time in the ‘irrigation-
270 stop’ plots was analyzed by testing for a difference between irrigated and the irrigation-stop in
271 a mixed effect model. Treatment and month were fixed factors, and tree nested in date was
272 treated as a random factor. Using the ‘multcomp’ package in R (Hothorn *et al.*, 2019), pairwise
273 comparisons per date were visualized.

274 **Results**

275 *Climate*

276 Volumetric soil water content at 10 and 80 cm depth was significantly higher in the irrigated
277 plots than in the control and irrigation-stop plots during the summer months when the irrigation
278 was activated (Fig. 2). From late autumn until spring, soil water content was comparable over
279 all treatments because the irrigation treatment was switched off. Natural precipitation events
280 (and failures in the irrigation system) during the summer months occasionally reduced the
281 treatment differences across soil depths. Mean daily VPD ranged from close to 0 in the winter
282 months to a maximum of 2.5 kPa in the dry and hot summer months.

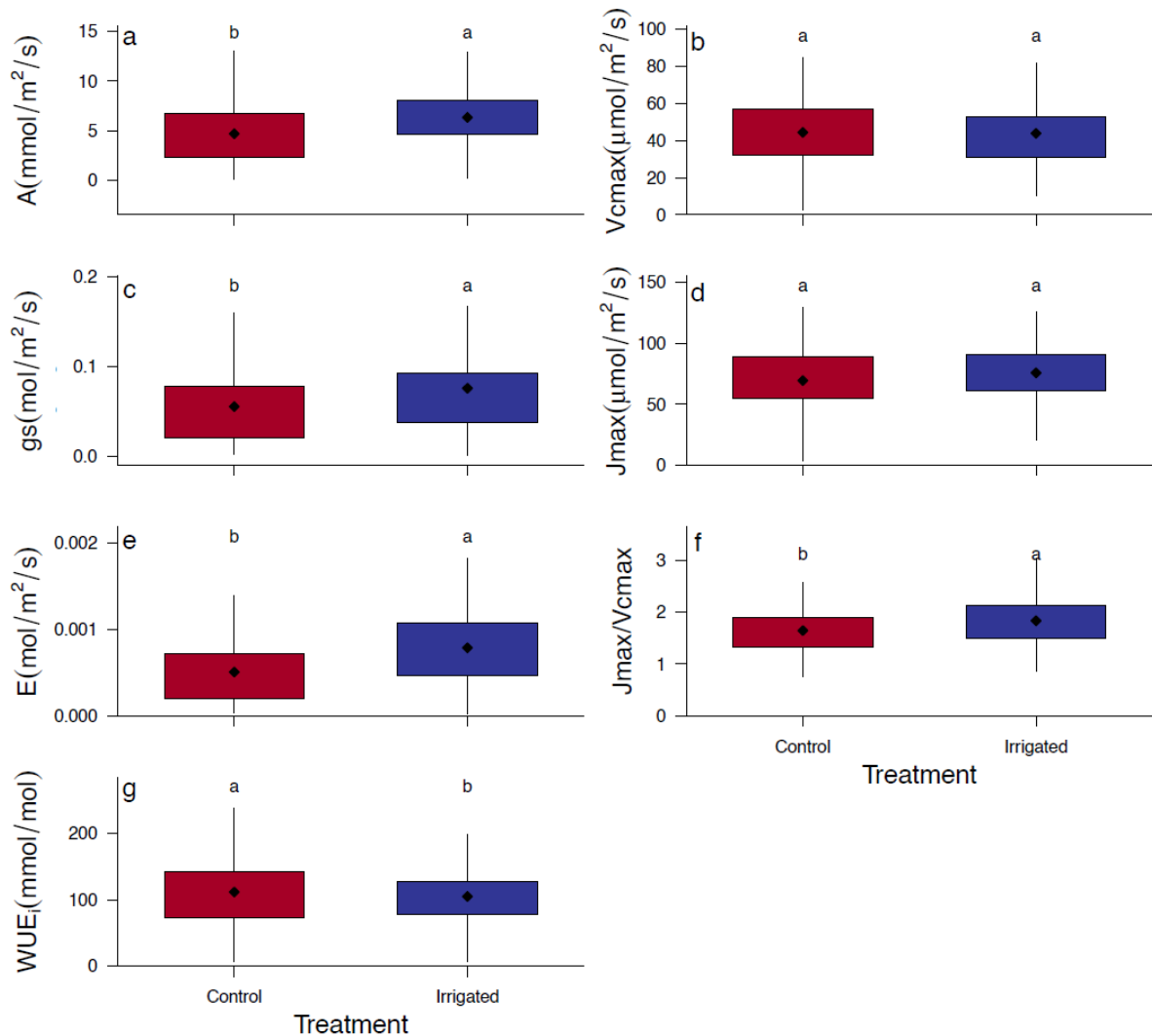


283

284 **Figure 2:** (a) Daily means of vapor pressure deficit (VPD), (b) maximum daily temperatures, and (c)
 285 differences in daily volumetric soil water content (VWC) between control and irrigated (blue), and
 286 control and irrigation-stop plots (orange). Solid lines show soil VWC at 10 cm depth and dashed lines
 287 at 80 cm depth. Grey vertical dashed lines indicate the dates when gas exchange measurement campaigns
 288 were conducted.

289 *Acclimation to long-term environmental conditions*

290 Irrigated trees showed in general higher g_s (60% increase, $p < 0.001$), A (34% increase, $p <$
 291 0.001) and E (60% increase, $p < 0.001$) than control trees after the 11-year acclimation period
 292 (Fig. 3, Table S2). WUE_i was only slightly lower in irrigated than in control trees (6%
 293 difference, $p=0.04$) and no significant treatment difference was found for $V_{c_{max}}$, ($C = 44.4 \pm$
 294 2.14 vs. 43.9 ± 1.7) and J_{max} ($C = 69.4 \pm 2.9$ vs. $I = 75.8 \pm 2.5$), while the ratio between the two
 295 ($J_{max}/V_{c_{max}}$) was marginally higher in irrigated trees compared to control trees ($C = 1.6 \pm 0.05$
 296 vs. $I = 1.8 \pm 0.06$) (Fig. 3, Table S2).

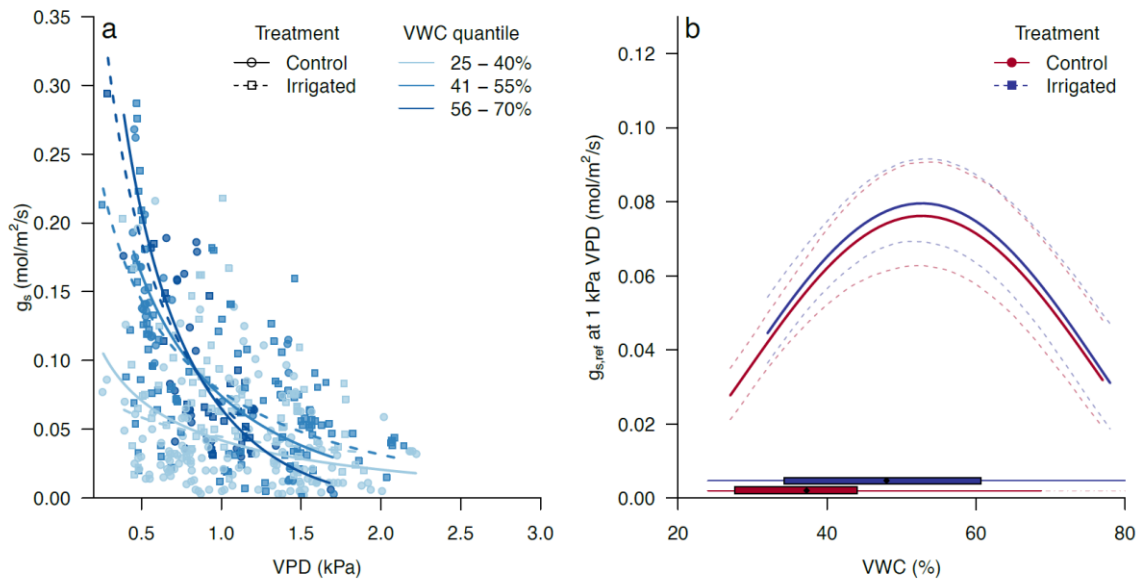


297

298 **Figure 3:** Treatment differences for photosynthesis (A), stomatal conductance (g_s), transpiration (E),
 299 intrinsic water use efficiency (WUE_i), $V_{c_{max}}$, and J_{max} and the ratio between the two as an average of all
 300 measurements between 2013 and 2019 in control / natural dry (red) and irrigated (blue) trees. Symbols
 301 show the mean; boxes and whiskers the interquartile ± 1.5 * interquartile range. Different letters above
 302 the boxplots indicate significant group differences according to linear mixed effect models ($p < 0.05$).

303 *Sensitivity of g_s to short-term environmental changes*

304 A strong logarithmic relationship was found between g_s and VPD (Fig. 4a). The long-term
 305 acclimation of the trees affected g_s ' sensitivity (i.e., m , the slope of the curve) to short-term
 306 fluctuations in VPD. With increasing VPD, control trees reduced g_s faster than irrigated trees
 307 (Fig. 4a; Table S3, S4). This treatment difference was most pronounced in low and intermediate
 308 soil VWC (25 – 55% VWC) (Supporting information Fig. S2). Soil drying below 55% VWC
 309 resulted in a decrease of $g_{s,ref}$ for both treatments (Fig. 4b).

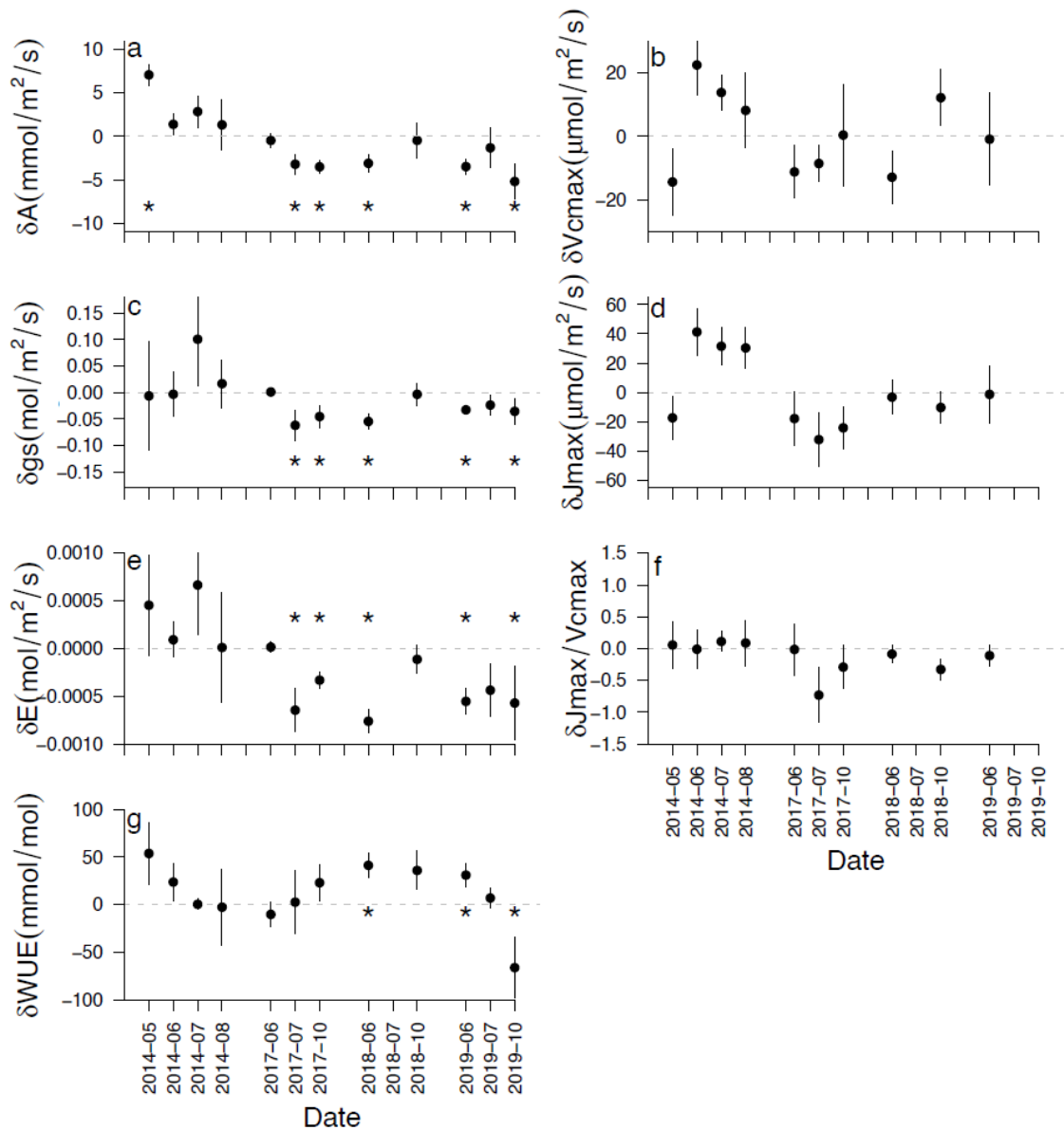


310

311 **Figure 4:** a) Stomatal conductance (g_s) vs. vapor pressure deficit (VPD). Colors show fitted model
 312 regressions according to the linear mixed effect model, per volumetric soil water content (VWC)
 313 quantile. Line type distinguishes control and irrigated treatments. b) $g_{s,\text{ref}}$ (g_s at 1 kPa VPD) as a function
 314 of soil VWC per treatment according to the linear mixed effect model. Colors indicate control and
 315 irrigated treatments. Dashed lines show the 95% credibility intervals of the mixed effect model. The
 316 range distribution of soil VWC in control and irrigated plots is shown on the bottom of the graph for
 317 reference.

318 *Acclimation over time after irrigation-stop*

319 During 2014, the year of the irrigation-stop, assimilation did not decline significantly in the
 320 irrigation-stop trees compared to irrigated trees (Fig. 5, Supporting information Fig. S3). In
 321 spring 2014, A , $V_{c_{\text{max}}}$ and J_{max} were even higher in irrigation-stop trees than in irrigated trees.
 322 From 2017 onwards, A , g_s , and E were significantly lower in irrigation-stop than irrigated trees
 323 (Fig. 5) and had reduced significantly compared to 2014 (Supporting information Fig. S3;
 324 Supporting information Table S2). Water use efficiency showed a steady increase from 2017 to
 325 2019; both compared to irrigated trees and in absolute terms (Fig. 5, Supporting information
 326 Fig. S3). $V_{c_{\text{max}}}$ and J_{max} dropped from being higher than irrigated trees in 2014 to lower or
 327 comparable in 2017. $V_{c_{\text{max}}}$ recovered to original levels in 2018 and 2019. The ratio between
 328 J_{max} and $V_{c_{\text{max}}}$ decreased between 2014 and 2019 steadily but not significantly.



329

330 **Figure 5.** Differences between ‘irrigation-stop’ and irrigated trees at four measuring campaigns in 2014
 331 and three in each year of 2017, 2018 and 2019. Plots show photosynthesis (a), stomatal conductance
 332 (g_s) (c), transpiration (E) (e), intrinsic water use efficiency (WUE) (g), V_{cmax} (b) and J_{max} (d), and the
 333 ratio between the two (f). Symbols indicate the difference of the two means (irrigation-stop minus
 334 irrigated) and error bars the SE of the mean differences. Asterisks indicate significant differences
 335 between irrigated and irrigation-stop trees ($p < 0.05$). Data is missing in 2018-07 due to technical
 336 problems resulting in a low number of tree replicates and absence of measurements on irrigation-stop
 337 trees. A/Ci parameters are missing in July and October 2019, when only point measurements were taken.

338 Discussion

339 Long-term acclimation to environmental conditions

340 Our hypothesis that irrigated trees had lower water use efficiency (WUE_i), and similar
 341 photosynthesis (A), stomatal conductance (g_s), evaporation (E), V_{cmax} and J_{max} was confirmed

342 for $V_{c_{max}}$ and J_{max} , and very weakly for WUE_i , while A , g_s , and E were even higher in irrigated
343 than control trees. Since the start of irrigation in 2003, irrigated trees have increased total leaf
344 area compared to the control trees (Schönbeck *et al.*, 2018). The higher assimilation rates
345 together with structural acclimation suggest an even higher C turnover than expected in
346 irrigated compared to control trees. The differences in gas exchange parameters are relatively
347 small, even though they are statistically significant, which is probably caused by these structural
348 adjustments in the canopy, which reduces the need for large assimilation increases and limits
349 the variation in WUE_i between control and irrigated trees (Cinnirella *et al.*, 2002). A smaller
350 crown (lower total leaf area) reduces the total water loss and reduces the need for leaf-level
351 water-conserving strategies such as increasing WUE_i (Cinnirella *et al.*, 2002; McDowell *et al.*,
352 2002). The fact that A and g_s were higher but $V_{c_{max}}$ and J_{max} were similar in irrigated compared
353 to control trees suggests a strong stomatal control of photosynthesis (Zhou *et al.*, 2013), with a
354 smaller role for, and potential acclimation of, Rubisco activity (Parry, 2002), electron transport
355 capacity (Epron and Dreyer, 1992) or mesophyll conductance (Egea *et al.*, 2011). This
356 speculation is corroborated by the fact that nitrogen concentration in the leaves, an essential
357 component of Rubisco, did not change with irrigation (Schönbeck *et al.*, 2018).

358 *Short-term sensitivity as affected by long-term acclimation to artificial change*

359 We expected a higher sensitivity of g_s to VPD and soil VWC fluctuations in irrigated trees
360 compared to control trees. Instead, control trees showed a higher sensitivity of g_s to increasing
361 VPD. These results suggest that atmospheric constraints may play a more critical and
362 increasingly important role in trees exposed to soil drought than trees growing in wetter soil
363 conditions. This is in contradiction with a study by Novick *et al.* (2016), who predicted a smaller
364 role for VPD limitation in soil moisture limited biomes. However, it is important to note that in
365 our study, no comparison is made between biomes but between trees that have been exposed to
366 a number of severe droughts in the last two decades, and trees that have been released from
367 these drought episodes. Control trees constantly operate at significantly lower soil VWC than
368 irrigated trees (37% vs. 48% resp., Fig. 4b). Although structural acclimation – i.e. smaller leaf
369 area compared to irrigated trees – should reduce whole-tree transpiration and thus water demand
370 of the control tree compared to irrigated trees, needle water potentials measured in 2016 show
371 that control trees do experience lower water potentials and hence drought stress (Schönbeck *et al.*
372 *et al.*, 2018). *Pinus sylvestris* is an isohydric species, indicating a strong control of stomatal
373 conductance with increasing VPD (Meinzer *et al.*, 2009; Martínez-Sancho *et al.*, 2017). In
374 analyses of whole-tree sap flow, Grossiord *et al.* (2018) found similar sensitivity of sap flow in
375 control and irrigated trees to VPD. However, they defined sensitivity only by the maximum sap

376 flux density at optimal VPD, which is more comparable to $g_{s,ref}$. We do agree that this influences
377 the sensitivity curve. Still, we think that the sensitivity parameter m , which is significantly
378 different between treatments in our study does indicate a higher sensitivity of g_s to VPD in
379 control trees. It should be noted that extrapolation from the needle-level to the crown is very
380 complex, and we do state that in our study, the highest strength lies in determining leaf-level
381 photosynthetic characteristics. The sensitivity of g_s to soil VWC changes is well reported in
382 other studies that show that soil drying reduces $g_{s,ref}$ (Schäfer, 2011). For control trees, this
383 means that they can keep their physiological potential to exploit ‘windows of opportunities’ –
384 i.e. times when water is available in higher amounts. Such rapid responses to precipitation were
385 demonstrated by Joseph et al. (2020), who found a strong increase in carbon allocation to
386 belowground tissues in the control plots of the same forest system after a precipitation event.

387 *Acclimation to sudden long-term changes in precipitation*

388 Against our expectation, the stop of irrigation did not reduce any leaf-level gas exchange
389 parameter in the first year, 2014 in relation to the irrigated trees (Fig. 5), despite rapid reductions
390 in the soil available water (Fig. 2). Instead, irrigation-stop trees kept similar g_s , E , and A as
391 irrigated trees. A slight reduction in A and E was observed between May and August 2014. It
392 should be noted that the treatment differences in soil VWC became apparent only in June 2014.
393 It is thus logical to expect no treatment differences in May 2014 yet. Irrigation-stop trees had
394 even higher A than irrigated trees in May 2014. Over the summer months, the continued high
395 evaporation rates and stomatal conductance could have translated into even lower soil VWC in
396 the irrigation-stop plots than in control plots from July 2014 onwards. These findings do not
397 fully correspond to the results of a study on sap flow and tree water deficit by Zweifel *et al.*
398 (2020). They found a gradual decrease of whole tree sap flow rates over the season and even
399 lower values than control trees from June onwards. Whole-tree sap flow measurements are a
400 result of transpiration of the entire crown. In our study, we always measured needles that
401 emerged in the previous year. Thus, a significant physiological and morphological difference
402 between newly emerged needles and the older cohorts was created during the year 2014. Indeed,
403 Zweifel *et al.* (2020) show that needle length decreased to levels below those of control trees,
404 significantly reducing the total leaf area of the tree. Several studies show large differences
405 between needle cohorts in coniferous species (Jach and Ceulemans, 2000; Robakowski and
406 Bielinis, 2017), and as the year advances towards the end of the growing season, current year
407 needles become increasingly important for tree productivity (Jensen *et al.*, 2015). The steep
408 reduction in the newly formed leaf area could have had significant impacts on the whole crown

409 transpiration, while the older needle cohorts did not react to the changes in soil VWC yet.
410 Similar findings were reported

411 Three years after the halt of irrigation, A, g_s , and E had dropped below the levels of irrigated
412 trees and remained lower for most measuring dates until the end of 2019. Water use efficiency
413 showed a gradual increase over time until 2018 and dropped again in 2019. The slow process
414 of increasing WUE_i is surprising; however, it is a sign for a conservative but very plastic
415 acclimation strategy of pine (Zweifel and Sterck, 2018). WUE_i is highly variable over the
416 season, but an average increase of WUE_i relative to irrigated trees was expected in the first few
417 needle cohorts. Instead, WUE_i in irrigation-stop trees was higher than in irrigated trees for the
418 first time in June 2018 (measured on the needle cohort emerging in 2017). It appears that the
419 characteristics of newly built tree structures are programmed not only by current conditions but
420 also by a certain ecological memory effect, which limits the range of adjustments of trees to
421 environmental changes (Anderegg *et al.*, 2018; Zweifel *et al.*, 2020).

422 Apparent J_{max} and $V_{c_{max}}$ had also dropped (Supporting information Fig. S3) to slightly lower
423 levels compared to irrigated trees (Fig. 5) but seemed to have recovered in 2018 again. While
424 it was expected for A, g_s , and E, the effects of drought on apparent $V_{c_{max}}$ and apparent J_{max} are
425 far less understood. These results indicate that both stomatal/diffusional limitations and
426 biochemical limitations inhibited photosynthesis in 2017. Decreases of J_{max} have been observed
427 for plant species across many ecosystems (Nogués and Baker, 2000; Ogaya and Peñuelas, 2003;
428 Pezner *et al.*, 2020), suggesting that many species experience a downregulation of electron
429 transport in response to drought. Interestingly, apparent $V_{c_{max}}$ and, in a lesser amount, apparent
430 J_{max} show a recovery over the years 2017-2019. Such a recovery was also found in some other
431 species (Pankovic *et al.*, 1999; Damour *et al.*, 2009; Zhou *et al.*, 2016) and could be a result of
432 structural acclimation to drought during the three years of irrigation-stop, allowing for higher
433 ‘per-leaf-area’ gas exchange rates (McDowell *et al.*, 2002; Schönbeck *et al.*, 2018). For Scots
434 pine, a full adjustment of the crown would take approximately 3-5 years, corresponding to the
435 total number of needle cohorts from a tree crown (Zweifel *et al.*, 2020). This shows that the
436 photosynthetic capacity on a biochemical level has recovered so that ‘windows of opportunity’
437 can be fully optimized, while on average, leaf-level A, E, and g_s remain low – i.e. comparable
438 to control trees.

439 This study was carried out over seven years, which creates a highly needed long-term
440 perspective of leaf acclimation to changing environmental conditions. It highlights the
441 importance of understanding leaf structure and biochemical composition to better extrapolate

442 whole-tree water and carbon dynamics. Compared to other spatially large-scale studies, the
443 results show that more knowledge is needed on between-needle-cohort differences in structure
444 and function to translate these results to whole-crown or whole-tree hydraulics and carbon
445 dynamics. Nevertheless, this unique experiment offers a detailed overview of needle structure
446 and function across various environmental conditions.

447 Multi-year records of gas exchange at the individual tree-level in the same forest ecosystem are
448 rare, and studies often focus either on short-term treatment effects or steady-state natural
449 conditions. Nevertheless, long-term measurements are indispensable to distinguish intraspecific
450 differences in photosynthesis capacity and sensitivity (Bachofen et al., 2020) and much of the
451 uncertainty in projecting future terrestrial carbon uptake and storage is due to a lack of
452 knowledge of the long-term response of photosynthetic carbon assimilation to future conditions
453 (Friedlingstein *et al.*, 2014). With this long-term irrigation manipulation experiment in a natural
454 forest, we studied the sensitivity to short-term environmental changes depending on long-term
455 acclimation to soil water availability. We found that long-term acclimation to increased soil
456 VWC has increased C assimilation on the leaf-level, which in combination with higher leaf area
457 caused an increased C assimilation on the whole tree-level. This larger crown does not seem to
458 make the leaves more sensitive to changes in atmospheric demand. Instead, drought release
459 reduced the sensitivity of stomata to increasing VPD. Lastly, understanding how structural and
460 biochemical adjustments occur due to environmental changes over time is indispensable for
461 future predictions of how forests react to a changing climate. Thus, our findings that structural
462 adjustments lead to an attenuation of initially strong leaf-level acclimation to strong multiple-
463 year drought shed a new and important light on the memory effects and acclimation potential
464 of evergreen trees to sudden environmental changes. The acclimation pathways found in this
465 study are limited to a single pine species but are expected to be valid to a range of evergreen
466 conifers, while research on deciduous species would greatly enhance our knowledge on the
467 acclimation potential of forests all around the world.

468 **Acknowledgements**

469 This study is based on data from the long-term Pfywald irrigation experiment, which is part
470 of the Swiss Long-term Forest Ecosystem Research Program LWF (www.lwf.ch). We thank
471 Christian Hug, Peter Bleuler, Simpal Kumar, Peter Jakob, Matthias Häni, and Flurin Sutter for
472 their continuing support on-site, for data preparation, and the fruitful discussions. A.G. and C.G.
473 acknowledge support from the Swiss National Science Foundation SNF (310030_189109 and
474 PZ00P3_174068). Y.S. acknowledges support from NERC (RA0929) and the Finnish Academy

475 (323843). Furthermore, we acknowledge the long-term help by Konrad Egger and his team
476 from the Forstrevier Leuk, the Burgerschaft Leuk, and the HYDRO Exploitation SA.

477 **Author contributions**

478 A.R., A.G., M.S., Y.S., and L.S. designed the experiment. M.S., Y.S., L.S., J.G. and P.D. carried
479 out gas exchange measurements, K.M. and R.Z. were responsible for continuous soil and
480 meteorological data acquisition and cleaning. L.S., C.G. and B.S. analyzed the data and L.S.
481 wrote the manuscript. All authors contributed to the interpretation and writing of the
482 manuscript.

483 **Data availability**

484 The data that support the findings of this study are available from the corresponding author
485 upon reasonable request.

486 **References**

487 **Allen CD, Macalady AK, Chenchouni H, et al.** 2010. A global overview of drought and
488 heat-induced tree mortality reveals emerging climate change risks for forests. *Forest Ecology*
489 *and Management* **259**, 660–684.

490 **Anderegg WRL, Wolf A, Arango-Velez A, et al.** 2018. Woody plants optimise stomatal
491 behaviour relative to hydraulic risk. *Ecology Letters* **21**, 968–977.

492 **Bachofen C, D’Odorico P, Buchmann N.** 2020. Light and VPD gradients drive foliar
493 nitrogen partitioning and photosynthesis in the canopy of European beech and silver fir.
494 *Oecologia* **192**, 323–339.

495 **Bigler C, Bräker OU, Bugmann H, Dobbertin M, Rigling A.** 2006. Drought as an inciting
496 mortality factor in Scots pine stands of the Valais, Switzerland. *Ecosystems* **9**, 330–343.

497 **Brandes E, Kodama N, Whittaker K, Weston C, Rennenberg H, Keitel C, Adams MA,**
498 **Gessler A.** 2006. Short-term variation in the isotopic composition of organic matter allocated
499 from the leaves to the stem of *Pinus sylvestris*: effects of photosynthetic and
500 postphotosynthetic carbon isotope fractionation. *Global Change Biology* **12**, 1922–1939.

501 **Brunner I, Graf Pannatier E, Frey B, Rigling A, Landolt W, Zimmermann S, Dobbertin**
502 **M.** 2009. Morphological and physiological responses of Scots pine fine roots to water supply
503 in a dry climatic region in Switzerland. *Tree Physiology* **29**, 541–550.

504 **von Caemmerer S, Farquhar GD.** 1981. Some relationships between the biochemistry of
505 photosynthesis and the gas exchange of leaves. *Planta* **153**, 376–387.

506 **Castrillo M, Fernandez D, Calcagno AM, Trujillo I, Guenni L.** 2001. Responses of
507 Ribulose-1,5-Bisphosphate Carboxylase, Protein Content, and Stomatal Conductance to
508 Water Deficit in Maize, Tomato, and Bean. *Photosynthetica* **39**, 221–226.

509 **Cinnirella S, Magnani F, Saracino A, Borghetti M.** 2002. Response of a mature *Pinus*
510 *laricio* plantation to a three-year restriction of water supply: structural and functional
511 acclimation to drought. *Tree Physiology* **22**, 21–30.

512 **Critchfield WB, Little EL.** 1966. *Geographic distribution of the pines of the world* /.
513 Washington, D.C. : U.S. Dept. of Agriculture, Forest Service,.

514 **Damour G, Vandame M, Urban L.** 2009. Long-term drought results in a reversible decline
515 in photosynthetic capacity in mango leaves, not just a decrease in stomatal conductance. *Tree*
516 *Physiology* **29**, 675–684.

517 **Dobbertin M, Eilmann B, Bleuler P, Giuggiola A, Graf Pannatier E, Landolt W,**
518 **Schleppi P, Rigling A.** 2010. Effect of irrigation on needle morphology, shoot and stem
519 growth in a drought-exposed *Pinus sylvestris* forest. *Tree Physiology* **30**, 346–360.

520 **Duursma RA.** 2015. *Plantecophys - An R Package for Analysing and Modelling Leaf Gas*
521 *Exchange Data* (PC Struik, Ed.). *PLOS ONE* **10**, e0143346.

522 **Egea G, Verhoef A, Vidale PL.** 2011. Towards an improved and more flexible
523 representation of water stress in coupled photosynthesis–stomatal conductance models.
524 *Agricultural and Forest Meteorology* **151**, 1370–1384.

525 **Epron D, Dreyer E.** 1992. Effects of severe dehydration on leaf photosynthesis in *Quercus*
526 *petraea* (Matt.) Liebl.: photosystem II efficiency, photochemical and nonphotochemical
527 fluorescence quenching and electrolyte leakage. *Tree Physiology* **10**, 273–284.

528 **Farquhar GD, von Caemmerer S, Berry JA.** 1980. A biochemical model of photosynthetic
529 CO₂ assimilation in leaves of C₃ species. *Planta* **149**, 78–90.

530 **Flexas J, Bota J, Loreto F, Cornic G, Sharkey TD.** 2004. Diffusive and Metabolic
531 Limitations to Photosynthesis under Drought and Salinity in C₃ Plants. *Plant Biology* **6**, 269–
532 279.

533 **Friedlingstein P, Meinshausen M, Arora VK, Jones CD, Anav A, Liddicoat SK, Knutti**
534 **R.** 2014. Uncertainties in CMIP5 Climate Projections due to Carbon Cycle Feedbacks.
535 *Journal of Climate* **27**, 511–526.

536 **Gelman A, Su Y-S, Yajima M, Hill J, Pittau MG, Kerman J, Zheng T, Dorie V.** 2020.

537 Package ‘arm’. R topics documented.

538 **Gessler A, Schaub M, McDowell NG.** 2017. The role of nutrients in drought-induced tree
539 mortality and recovery. *New Phytologist* **214**, 513–520.

540 **Gimmi U, Wohlgemuth T, Rigling A, Hoffmann CW, Bürgi M.** 2010. Land-use and
541 climate change effects in forest compositional trajectories in a dry Central-Alpine valley.
542 *Annals of Forest Science* **67**, 701–701.

543 **Grossiord C, Buckley TN, Cernusak LA, Novick KA, Poulter B, Siegwolf RTW, Sperry
544 JS, McDowell NG.** 2020. Plant responses to rising vapor pressure deficit. *New Phytologist*,
545 *nph.16485*.

546 **Grossiord C, Sevanto S, Limousin JM, Meir P, Mencuccini M, Pangle RE, Pockman
547 WT, Salmon Y, Zweifel R, McDowell NG.** 2018. Manipulative experiments demonstrate
548 how long-term soil moisture changes alter controls of plant water use. *Environmental and
549 Experimental Botany* **152**, 19–27.

550 **Gu L, Pallardy SG, Tu K, Law BE, Wullschleger SD.** 2010. Reliable estimation of
551 biochemical parameters from C3 leaf photosynthesis-intercellular carbon dioxide response
552 curves. *Plant, Cell & Environment* **33**, 1852–1874.

553 **Hommel R, Siegwolf R, Saurer M, Farquhar GD, Kayler Z, Ferrio JP, Gessler A.** 2014.
554 Drought response of mesophyll conductance in forest understory species - impacts on water-
555 use efficiency and interactions with leaf water movement. *Physiologia Plantarum* **152**, 98–
556 114.

557 **Hothorn T, Bretz F, Westfall P, Heiberger RM, Schuetzenmeister A, Scheibe S.** 2019.
558 Package ‘multcomp’. R topics documented.

559 **Jach ME, Ceulemans R.** 2000. Effects of season, needle age and elevated atmospheric CO2
560 on photosynthesis in Scots pine (*Pinus sylvestris*). *Tree Physiology* **20**, 145–157.

561 **Jensen AM, Warren JM, Hanson PJ, Childs J, Wullschleger SD.** 2015. Needle age and
562 season influence photosynthetic temperature response and total annual carbon uptake in
563 mature *Picea mariana* trees. *Annals of Botany* **116**, 821–832.

564 **Joseph J, Gao D, Backes B, et al.** 2020. Rhizosphere activity in an old-growth forest reacts
565 rapidly to changes in soil moisture and shapes whole-tree carbon allocation. *Proceedings of
566 the National Academy of Sciences* **117**, 24885–24892.

567 **Kanechi M, Uchida N, Yasuda T, Yamaguchi T.** 1996. Non-Stomatal Inhibition Associated

568 with Inactivation of Rubisco in Dehydrated Coffee Leaves under Unshaded and Shaded
569 Conditions. *Plant and Cell Physiology* **37**, 455–460.

570 **De Kauwe MG, Medlyn BE, Zaehle S, et al.** 2013. Forest water use and water use efficiency
571 at elevated CO₂: a model-data intercomparison at two contrasting temperate forest FACE
572 sites. *Global Change Biology* **19**, 1759–1779.

573 **Keenan T, Sabate S, Gracia C.** 2010. Soil water stress and coupled photosynthesis-
574 conductance models: Bridging the gap between conflicting reports on the relative roles of
575 stomatal, mesophyll conductance and biochemical limitations to photosynthesis. *Agricultural
576 and Forest Meteorology* **150**, 443–453.

577 **Kelly JWG, Duursma RA, Atwell BJ, Tissue DT, Medlyn BE.** 2016. Drought × CO₂
578 interactions in trees: a test of the low-intercellular CO₂ concentration (C_i) mechanism. *New
579 Phytologist* **209**, 1600–1612.

580 **Kozłowski T, Pallardy S.** 2002. Acclimation and adaptive responses of woody plants to
581 environmental stresses. *The Botanical Review* **68**, 270–334.

582 **Kuznetsova A, Brockhoff P, Christensen R.** 2017. lmerTest package: Tests in linear mixed
583 effects models. *Journal of Statistical software* **82**, 1–26.

584 **Marchin RM, Broadhead AA, Bostic LE, Dunn RR, Hoffmann WA.** 2016. Stomatal
585 acclimation to vapour pressure deficit doubles transpiration of small tree seedlings with
586 warming. *Plant, Cell & Environment* **39**, 2221–2234.

587 **Martínez-Sancho E, Vásconez Navas LK, Seidel H, Dorado-Liñán I, Menzel A.** 2017.
588 Responses of Contrasting Tree Functional Types to Air Warming and Drought. *Forests* **8**,
589 450.

590 **Martínez-Vilalta J, Cochard H, Mencuccini M, et al.** 2009. Hydraulic adjustment of Scots
591 pine across Europe. *New Phytologist* **184**, 353–364.

592 **McDowell N, Barnard H, Bond B, et al.** 2002. The relationship between tree height and leaf
593 area: sapwood area ratio. *Oecologia* **132**, 12–20.

594 **Medlyn BE, Loustau D, Delzon S.** 2002. Temperature response of parameters of a
595 biochemically based model of photosynthesis. I. Seasonal changes in mature maritime pine
596 (*Pinus pinaster* Ait.). *Plant, Cell and Environment* **25**, 1155–1165.

597 **Meinzer FC, Johnson DM, Lachenbruch B, McCulloh KA, Woodruff DR.** 2009. Xylem
598 hydraulic safety margins in woody plants: coordination of stomatal control of xylem tension

599 with hydraulic capacitance. *Functional Ecology* **23**, 922–930.

600 **Nogués S, Baker NR.** 2000. Effects of drought on photosynthesis in Mediterranean plants
601 grown under enhanced UV-B radiation. *Journal of Experimental Botany* **51**, 1309–1317.

602 **Novick KA, Ficklin DL, Stoy PC, et al.** 2016. The increasing importance of atmospheric
603 demand for ecosystem water and carbon fluxes. *Nature Climate Change* **6**, 1023–1027.

604 **Ogaya R, Peñuelas J.** 2003. Comparative field study of *Quercus ilex* and *Phillyrea latifolia*:
605 photosynthetic response to experimental drought conditions. *Environmental and Experimental*
606 *Botany* **50**, 137–148.

607 **Oren R, Sperry JS, Katul GG, Pataki DE, Ewers BE, Phillips N, Schäfer KVR.** 1999.
608 Survey and synthesis of intra- and interspecific variation in stomatal sensitivity to vapour
609 pressure deficit. *Plant, Cell & Environment* **22**, 1515–1526.

610 **Palmroth S, Hari P.** 2001. Evaluation of the importance of acclimation of needle structure,
611 photosynthesis, and respiration to available photosynthetically active radiation in a Scots pine
612 canopy. *Canadian Journal of Forest Research* **31**, 1235–1243.

613 **Pankovic D, Sakac Z, Kevresan S, Plesnicar M.** 1999. Acclimation to long-term water
614 deficit in the leaves of two sunflower hybrids: photosynthesis, electron transport and carbon
615 metabolism. *Journal of Experimental Botany* **50**, 128–138.

616 **Parry MAJ.** 2002. Rubisco Activity: Effects of Drought Stress. *Annals of Botany* **89**, 833–
617 839.

618 **Pataki DE, Oren R, Phillips N.** 1998. Responses of sap flux and stomatal conductance of
619 *Pinus taeda* L. trees to stepwise reductions in leaf area. *Journal of Experimental Botany* **49**,
620 871–878.

621 **Pezner AK, Pivovarov AL, Sun W, Sharifi MR, Rundel PW, Seibt U.** 2020. Plant
622 functional traits predict the drought response of native California plant species. *International*
623 *Journal of Plant Sciences* **181**, 256–265.

624 **Poyatos R, Martínez-Vilalta J, Čermák J, et al.** 2007. Plasticity in hydraulic architecture of
625 Scots pine across Eurasia. *Oecologia* **153**, 245–259.

626 **Prentice IC, Dong N, Gleason SM, Maire V, Wright IJ.** 2014. Balancing the costs of
627 carbon gain and water transport: testing a new theoretical framework for plant functional
628 ecology (J Penuelas, Ed.). *Ecology Letters* **17**, 82–91.

629 **Renninger HJ, Carlo NJ, Clark KL, Schäfer KVR.** 2015. Resource use and efficiency, and

630 stomatal responses to environmental drivers of oak and pine species in an Atlantic Coastal
631 Plain forest. *Frontiers in Plant Science* **6**, 1–16.

632 **Rigling A, Bigler C, Eilmann B, et al.** 2013. Driving factors of a vegetation shift from Scots
633 pine to pubescent oak in dry Alpine forests. *Global Change Biology* **19**, 229–240.

634 **Robakowski P, Bielinis E.** 2017. Needle age dependence of photosynthesis along a light
635 gradient within an *Abies alba* crown. *Acta Physiologiae Plantarum* **39**, 83.

636 **Salmon Y, Lintunen A, Dayet A, Chan T, Dewar R, Vesala T, Hölttä T.** 2020. Leaf
637 carbon and water status control stomatal and nonstomatal limitations of photosynthesis in
638 trees. *New Phytologist* **226**, 690–703.

639 **Schäfer KVR.** 2011. Canopy Stomatal Conductance Following Drought, Disturbance, and
640 Death in an Upland Oak/Pine Forest of the New Jersey Pine Barrens, USA. *Frontiers in Plant*
641 *Science* **2**.

642 **Schönbeck L, Gessler A, Hoch G, McDowell NG, Rigling A, Schaub M, Li MH.** 2018.
643 Homeostatic levels of nonstructural carbohydrates after 13 yr of drought and irrigation in
644 *Pinus sylvestris*. *New Phytologist* **219**, 1314–1324.

645 **Serrano L, Gamon JA, Berry J.** 1997. Estimation of leaf area with an integrating sphere.
646 *Tree Physiology* **17**, 571–576.

647 **Sharkey TD, Bernacchi CJ, Farquhar GD, Singsaas EL.** 2007. Fitting photosynthetic
648 carbon dioxide response curves for C3 leaves. *Plant, Cell & Environment* **30**, 1035–1040.

649 **Simmons AJ, Willett KM, Jones PD, Thorne PW, Dee DP.** 2010. Low-frequency
650 variations in surface atmospheric humidity, temperature, and precipitation: Inferences from
651 reanalyses and monthly gridded observational data sets. *Journal of Geophysical Research* **115**,
652 D01110.

653 **Sultan SE.** 2000. Phenotypic plasticity for plant development, function and life history.
654 *Trends in Plant Science* **5**, 537–542.

655 **Tezara W.** 2002. Effects of water deficit and its interaction with CO₂ supply on the
656 biochemistry and physiology of photosynthesis in sunflower. *Journal of Experimental Botany*
657 **53**, 1781–1791.

658 **Thimonier A, Graf Pannatier E, Schmitt M, Waldner P, Walthert L, Schleppi P,**
659 **Dobbertin M, Kräuchi N.** 2010. Does exceeding the critical loads for nitrogen alter nitrate
660 leaching, the nutrient status of trees and their crown condition at Swiss Long-term Forest

661 Ecosystem Research (LWF) sites? *European Journal of Forest Research* **129**, 443–461.

662 **Thimonier A, Schmitt M, Waldner P, Rihm B.** 2005. Atmospheric deposition on Swiss
663 Long-Term Forest Ecosystem Research (LWF) plots. *Environmental Monitoring and*
664 *Assessment* **104**, 81–118.

665 **Wang H, Prentice IC, Keenan TF, Davis TW, Wright IJ, Cornwell WK, Evans BJ, Peng**
666 **C.** 2017. Towards a universal model for carbon dioxide uptake by plants. *Nature Plants* **3**,
667 734–741.

668 **Weber P, Rigling A, Bugmann H.** 2008. Sensitivity of stand dynamics to grazing in mixed
669 *Pinus sylvestris* and *Quercus pubescens* forests: A modelling study. *Ecological Modelling*
670 **210**, 301–311.

671 **Willett KM, Dunn RJH, Thorne PW, Bell S, de Podesta M, Parker DE, Jones PD,**
672 **Williams Jr. CN.** 2014. HadISDH land surface multi-variable humidity and temperature
673 record for climate monitoring. *Climate of the Past* **10**, 1983–2006.

674 **Wilson KB, Baldocchi DD, Hanson PJ.** 2000. Quantifying stomatal and non-stomatal
675 limitations to carbon assimilation resulting from leaf aging and drought in mature deciduous
676 tree species. *Tree Physiology* **20**, 787–797.

677 **Wright IJ, Reich PB, Westoby M.** 2003. Least-Cost Input Mixtures of Water and Nitrogen
678 for Photosynthesis. *The American Naturalist* **161**, 98–111.

679 **Wullschlegel SD.** 1993. Biochemical Limitations to Carbon Assimilation in C3 Plants—A
680 Retrospective Analysis of the A/C_i Curves from 109 Species. *Journal of Experimental*
681 *Botany* **44**, 907–920.

682 **Zhou S, Duursma RA, Medlyn BE, Kelly JWG, Prentice IC.** 2013. How should we model
683 plant responses to drought? An analysis of stomatal and non-stomatal responses to water
684 stress. *Agricultural and Forest Meteorology* **182–183**, 204–214.

685 **Zhou S-X, Medlyn BE, Prentice IC.** 2016. Long-term water stress leads to acclimation of
686 drought sensitivity of photosynthetic capacity in xeric but not riparian *Eucalyptus* species.
687 *Annals of Botany* **117**, 133–144.

688 **Zhou S, Medlyn B, Sabaté S, Sperlich D, Prentice IC, Whitehead D.** 2014. Short-term
689 water stress impacts on stomatal, mesophyll and biochemical limitations to photosynthesis
690 differ consistently among tree species from contrasting climates. *Tree Physiology* **34**, 1035–
691 1046.

692 **Zweifel R, Etzold S, Sterck F, et al.** 2020. Determinants of legacy effects in pine trees –
693 implications from an irrigation-stop experiment. *New Phytologist* **227**, 1081–1096.

694 **Zweifel R, Sterck F.** 2018. A Conceptual Tree Model Explaining Legacy Effects on Stem
695 Growth. *Frontiers in Forests and Global Change* **1**.

696